Natural Demodulation of 2D Fringe Patterns

Kieran G. Larkin

Canon Information Systems Research Australia Pty Ltd, 1 Thomas Holt Drive, North Ryde, Sydney, NSW 2113.

& Department of Physical Optics, School of Physics, The University of Sydney, NSW 2006, Australia.

Kieran.Larkin@physics.org

1 Introduction

For almost two decades one of the most successful methods of demodulating fringe patterns was based on the Fourier transform implementation of the 1-D Hilbert transform /1/ . Recently, however, a method of fringe analysis based on an isotropic 2-D Hilbert transform has been proposed /2/ . An isotropic Hilbert transform had been previously considered topologically impossible by many researchers. The new method has been called the "vortex transform" for brevity. The vortex transform [VT] is based on the approximate quadrature relationship of a spiral phase Fourier operator. The approximation is asymptotic /3/ with high accuracy predicted for any meaningful fringes; fringes which have a radius of curvature larger than the fringe spacing. An important aspect of the VT is the orientation phase factor required to obtain the final demodulated pattern's phase and amplitude. In this paper I shall concentrate on the remarkable simplification in fringe analysis made possible by the VT utilising orientation phase unwrapping.

In the mathematical sense, the spiral phase transform is revolutionary, but is it revolutionary in the sense of Kuhn /4/ who, in 1962, proposed "[Science] is a series of peaceful interludes punctuated by intellectually violent revolutions"? Some fierce opposition to the VT has already been encountered, so there is hope.

2 Two dimensional Fringe Patterns and the Vortex Operator

Consider a real 2D fringe pattern which already has the DC term removed (although this is an important pre-processing step the details are omitted here):

$$g(x,y) = b(x,y)\cos\left[\psi(x,y)\right]. \tag{1}$$

It is generally assumed that the amplitude and phase functions satisfy certain smoothness constraints which are consistent with most naturally occurring fringe patterns. The spiral phase quadrature transform is defined as a Fourier transform (FT), followed by a spiral phase multiplication, followed by an inverse FT. The FT is actually implemented on discrete data-sets (digital images) as a discrete Fast Fourier Transform (FFT). For simplicity the mathematical analysis is presented for 2D continuous functions, but the discrete implementation follows it rather closely with remarkably few edge, window, or leakage effects. The FT of the fringe pattern is defined by

$$G(u,v)=\int_{-\infty}^{+\infty}\int_{-\infty}^{+\infty} g(x,y)\exp\left(-2\pi i\left[ux+vy\right]\right)dxdy=\mathrm{F}\left\{g(x,y)\right\} \tag{2}$$

where $\mathrm{F}\{\ \}$ is the FT operator, (u,v) are the spatial frequency coordinate, and the Fourier polar coordinates (q,ϕ) are defined conventionally as $u=q\cos\phi,\quad v=q\sin\phi$.

Multiplying by a spiral Fourier phase function, and then transforming back gives the spiral phase quadrature transformation denoted here by the operator $\$\{\ \}$:

$$\begin{aligned}\$\left\{g(x,y)\right\}&=\mathrm{F}^{-1}\left\{\exp\left[i\phi(u,v)\right]\mathrm{F}\left\{b(x,y)\cos\left[\psi(x,y)\right]\right\}\right\}\\&\cong i\exp\left[i\beta(x,y)\right]b(x,y)\sin\left[\psi(x,y)\right].\end{aligned} \tag{3}$$

The crucial new parameter above is the fringe "orientation" $\beta=\beta(x,y)$. Jahne /5/ and other authors have defined the more useful and precise descriptors *direction* and *orientation*. They are distinguished by *direction* being a modulo 2π parameter, while *orientation* is a modulo π parameter. The *direction* is essentially a vector quantity and can be easily defined for gradients (especially phase gradients in our application). The *orientation* is more useful for local features such as fringes which are essentially unchanged by rotations of 180° (π radians). From here on Jahne's definitions will be used. Previous use of the phrase "unwrapped orientation" /2, 3, 6/ corresponds to the present term *direction*. Fig 1 is an illustration of direction versus orientation.

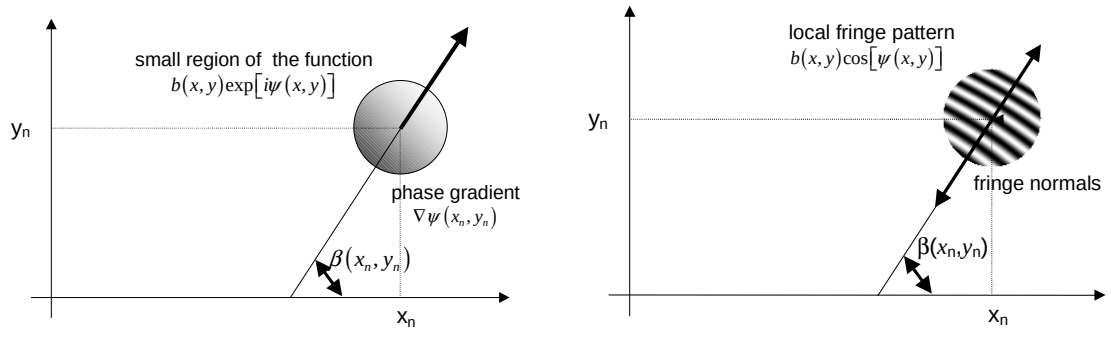

Fig 1(a) Definition of *direction* as phase gradient direction and, Fig 1(b) local fringe *orientation*.

Equation 3 has been verified (in the limit of infinitesimal fringe spacing) using stationary phase techniques. /3/ Crucially, again, the parameter β is shown to be the direction of the underlying phase gradient. The vortex transform V{}can be defined as follows:

$$\mathrm{V}\left\{g\right\}=-i\exp\left[-i\beta\right]\mathrm{F}^{-1}\left\{\exp\left[i\phi\right]\mathrm{F}\left\{g\right\}\right\}\simeq b(x,y)\sin\left[\psi(x,y)\right]. \tag{4}$$

The above result, although immensely powerful as part of a general 2D demodulation scheme, rather obscures some of the more subtle resolutions of classical problems in fringe analysis. These subtleties are also implicit (but obscured) in the stationary phase theory of the vortex transform /3/ . A recent paper of Bülow et al /7/ discusses a similar idea from the

perspective of the quaternionic Riesz transform whilst overlooking the literature on fringe analysis and phase unwrapping.

3 Local Analysis of Fringe Pattern

Although the VT is defined primarily by Fourier operators, it can also be represented (using the convolution theorem) as a 2D convolution (denoted by $**$) with a special complex kernel, followed by spatial domain multiplication

$$\mathrm{V}^{-1}\{g(x,y)\} = -i\exp\left[i\beta(x,y)\right]\left[g(x,y)**s(x,y)\right]. \tag{5}$$

Efficient space domain implementations can be expected to follow from the convolution property. The complex kernel has a spiral phase structure and an inverse square fall-off in magnitude:

$$s(x,y) = \frac{i(x+iy)}{2\pi\left(x^2+y^2\right)^{3/2}} = \frac{i\exp(i\theta)}{2\pi r^2} \tag{6}$$

An inverse square relation is favourable for compact kernel approximations. The local fringe pattern in a small region around a point (x_0, y_0) can be expanded as a Taylor series in partial phase derivatives $\psi_{m,n}$:

$$\psi(x_0+s, y_0+t) = \psi_{0,0}(x_0,y_0) + \psi_{1,0}(x_0,y_0)s + \psi_{0,1}(x_0,y_0)t + \ldots \tag{7}$$

Hence the locally straight fringe approximation arises from the a first order expansion:

$$\begin{aligned} g(x_0+s, y_0+t) &\simeq b_0\cos\left[\psi(x_0+s, y_0+t)\right] \\ &\simeq b_0\cos\left[\psi_{00}(x_0,y_0)\right]\cos\left[\psi_{10}(x_0,y_0)s + \psi_{01}(x_0,y_0)t\right] \\ &\quad - b_0\sin\left[\psi_{00}(x_0,y_0)\right]\sin\left[\psi_{10}(x_0,y_0)s + \psi_{01}(x_0,y_0)t\right]. \end{aligned} \tag{8}$$

A parametric form of the local fringe patterns could include direction angle β explicitly:

$$g_\beta(x_0+s, y_0+t) = b_0\cos\left[\psi_{00}(x_0,y_0) + q(x_0,y_0)\cos\beta(x_0,y_0)s + q(x_0,y_0)\sin\beta(x_0,y_0)t\right] \tag{9}$$

It is now clear that if the orientation is used instead of direction the value β may be in error by π, resulting in:

$$g_{\beta+\pi}(x_0+s, y_0+t) = g_\beta(x_0-s, y_0-t). \tag{10}$$

This equation may be simply interpreted as the local phase derivative of the fringe pattern swapping polarity. So it is not possible, using local properties alone, to distinguish real fringe patterns with opposite phase gradients. More simply, this ambiguity is a consequence of:

$$\cos\left[\psi(x,y)\right] = \cos\left[-\psi(x,y)\right]. \tag{11}$$

4 Illustration of Sidelobe Entanglement

Simple open fringe patterns give rise to Fourier sidelobes which are compact, diametrically opposite each other and well clear of the origin. Fig 2 shows a typical Fourier magnitude plot for the pattern of Fig 1(b).

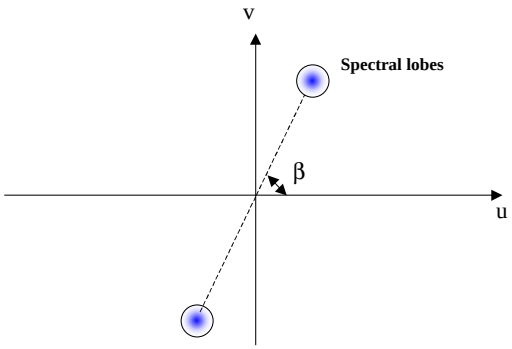

Figure 2, Spectral sidelobes of a simple open fringe pattern

It is quite straightforward to isolate the sidelobes and reverse polarity to obtain the quadrature fringe pattern in such a system. This explains the previous success of several ad-hoc schemes using oriented half-planes and quadrant "signum" functions for demodulating such patterns. If a closed fringe pattern is Fourier transformed, then the spectral lobes will be elongated into filaments which surround the origin. For a real fringe pattern there will be two filaments which inevitably overlap, often in an intricate manner. Figure 3(a) shows an ideal demodulated fringe pattern and Fig 3(b) its spectral magnitude which contains just one elongated sidelobe.

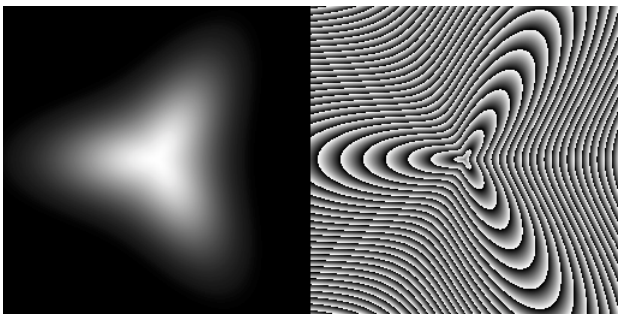

Fig 3(a) Complex fringe magnitude and phase

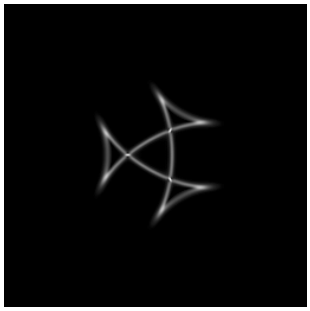

Fig 3(b) Spectrum

Consider Fig 4 which shows the real part of the complex fringe pattern and its spectrum. Because a cosine pattern contains two sidelobes compared to the complex exponential, which has only one sidelobe, we see overlapping and entangled sidelobes. The second sidelobe is a 180° rotated replica of the first sidelobe. The relative phase of the two sidelobes is controlled the cosine phase offset; in this particular case zero [equation (1)].

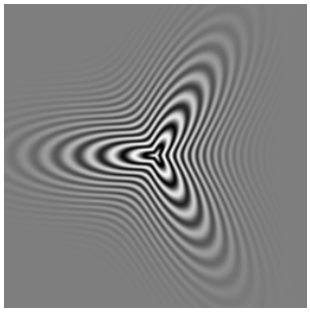

Fig 4(a) Real cosine fringe pattern

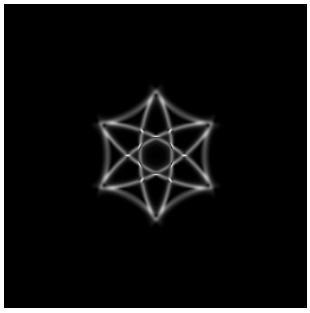

Fig 4(b) Spectrum: two tangled sidelobes

The overlap exhibited in Fig 4(b) clearly shows why Fourier-domain-only methods are incapable of the sidelobe separation implicitly required to reconstruct the complex exponenial fringe pattern of Fig 3. In short, no amount of filtering can separate or distinguish overlapping spectra.

So let's look at the problem again. The spiral phase transform brings us someway towards the goal of demodulation. In fact amplitude demodulation is trivial because equations (1) and (3) combine to give the modulus -squared amplitude:

$$\left|b(x,y)\right|^2 = \left|g(x,y)\right|^2 + \left|\$\{g(x,y)\}\right|^2 \tag{12}$$

5 Direction from Orientation Phase Unwrapping

5.1 Previous work

It should be mentioned that a number of other authors have noted the potential importance of fringe orientation in fringe analysis. Andresen and Yu /8/ proposed a directional filter or "spin filter" for adaptively enhancing fringes. Canabal et al /9/ presented a simple derivative method of estimating orientation which only fails at fringe peaks and valleys. In this example the fringe orientation was used directly to estimate the local refractive power of a lens. More recently Marroquin et al /10/ have described an essentially statistical technique of extracting fringe phase using estimates of the fringe orientation and direction. There is also a substantial body of literature on the subject of orientation estimation in the field of image processing and pattern analysis.

5.2 Conventional versus Orientational Phase Unwrapping

Various orientation detectors can recover an estimate of the double phase function $\exp\left[2i\beta(x,y)\right]$. This form essentially means that $\beta(x,y)$ is estimated modulo π. An estimate modulo 2π can be obtained by unwrapping the initial double phase function 2β modulo 4π then simply halving it. The unwrapping process for orientation has some peculiarities not well known in conventional 2D phase unwrapping:

- Firstly, the full range of unwrapped 2β is just 4π. Conventional unwrapping has no limit on the range and it is typically $\gg 4\pi$.

- Secondly, residues (or spiral singularities) are meaningful in orientation phase maps; they typically represent closed loop fringes. Other types of discontinuity, such as loops or

umbilics are possible (see Penrose for examples /11/) but are ignored here. Some conventional unwrapping techniques (such as those based upon the Fourier solution of the Poisson equation /12/) are "blind" to residues and therefore remove them from the unwrapped estimate.

5.3 Simple Direction Estimation Without Unwrapping

By utilising an orientation estimator based upon first and second partial derivatives the peak/valley problem evident in Canabal's work /9/ is avoided. When applied to the pattern in Fig 4(a) a double orientation map is obtained as shown in Fig 5(a). Note that the range is $-\pi \le 2\beta < \pi$. A simple direction estimate is obtained by halving the phase, as shown in Fig 5(b) with $-\pi/2 \le \beta < \pi/2$.

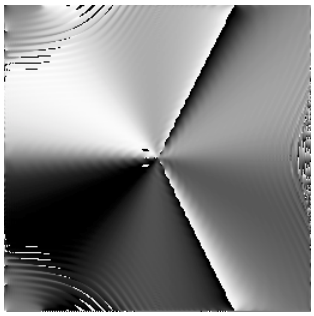

Fig 5(a) Orientation phase $-\pi \le 2\beta < \pi$

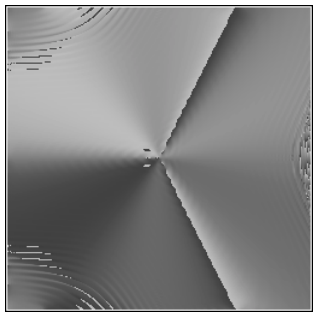

Fig 5(b) Simple direction phase $-\pi/2 \le \beta < \pi/2$

By demodulating the fringe pattern in Fig 4(a) with the simple direction map of Fig 5(b) a phase estimate is obtained which has occasional sign reversals in the quadrature component estimate, as shown in Fig 6(a), and in terms of magnitude and phase in Fig 6(b).

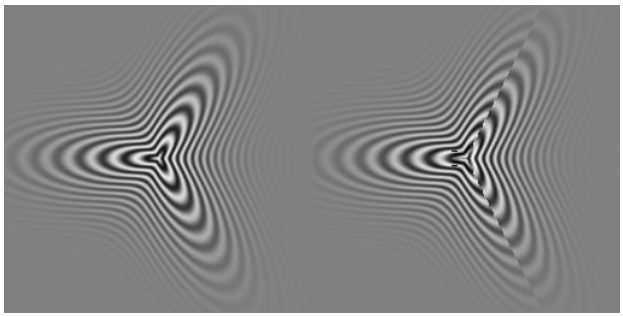

Fig 6 (a) The real and imaginary parts of a simple-direction-demodulated fringe pattern

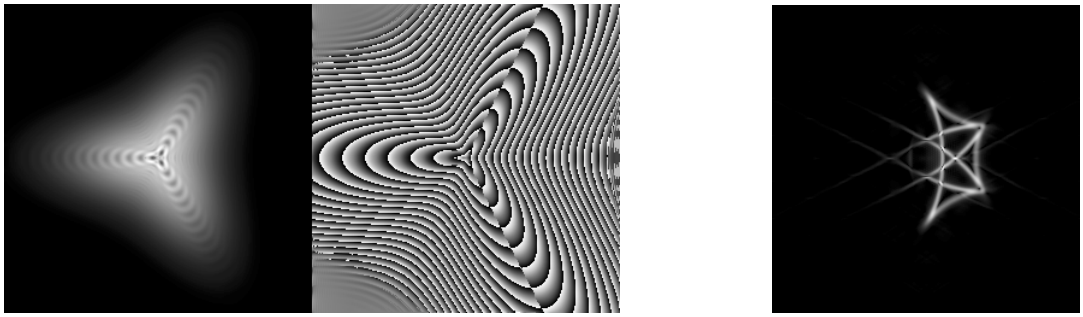

Fig 6 (b) The magnitude and phase of a simple-direction-demodulated fringe pattern and its spectrum

The spectrum shown in Fig 6(b) resembles the classical half-plane Hilbert transform spectrum, although the cut-off is not abrupt. The spectral leakage is related to the Fourier correspondence of the (desirable) sharp phase reversals in the demodulated fringe pattern.

5.4 Direction Estimation Using Phase Unwrapping

If instead of forming the simplistic direction estimate in the preceding section the unwrapping is such that $-2\pi \le 2\beta < 2\pi$, and by halving its value so that $-\pi \le \beta < \pi$, then the phase map shown in Fig 7 is obtained. Note the obvious first order spiral in the phase.

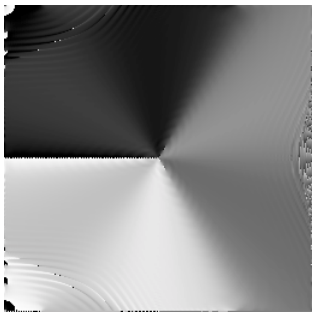

Fig 7 Direction map $-\pi \le \beta < \pi$ obtained from unwrapped orientation

Proceeding as before to demodulate the fringe pattern in Fig 4(a) but using the direction phase, a remarkably good estimate is obtained. The real and imaginary parts are shown in Fig 8(a), and the magnitude and phase in Fig 8(b).

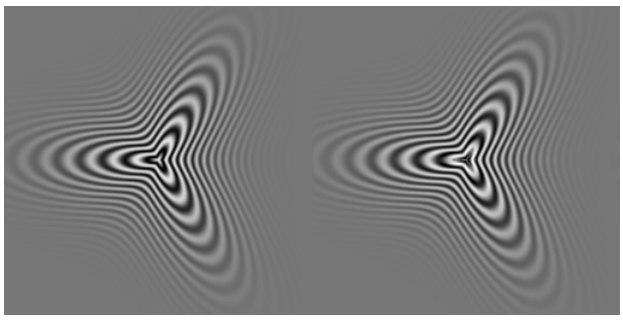

Fig 8(a) The real and imaginary parts of an unwrapped direction-demodulated fringe pattern

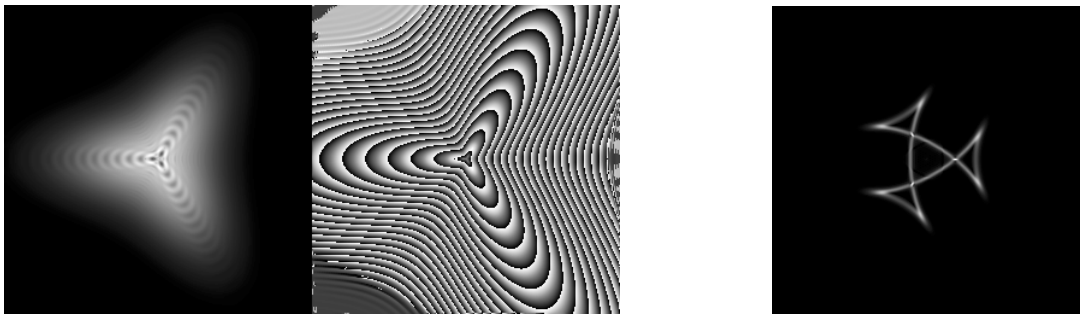

Fig 8(b) The magnitude and phase of an unwrapped direction-demodulated fringe pattern and its spectrum

Careful comparison of Fig 8(b) with the ideal phase pattern in Fig 3(a) shows a remarkable resemblance apart from a phase negation due to the global ambiguity in the fringe phase evident in equation(11). The final demodulated amplitude shows three radial lines with demodulation errors [the ideal magnitude is shown in Fig 3(a)] as predicted from the relative fringe curvature effect /3, 6/ . The fringe spacing in these regions is actually smaller than the radius of fringe curvature.

6 Acknowledgements

I would like to thank Don Bone for many insights into the problems of 2D demodulation. Michael Oldfield provided the friendly software for Fourier processing of complex images. Peter Fletcher drew my attention to the many details required for the demodulation of realistic and exquisitely convoluted fringe patterns such as fingerprints.

7 References

/1/ M. Takeda, H. Ina, and S. Kobayashi, "Fourier-transform method of fringe-pattern analysis for computer-based topography and interferometry", J. Opt. Soc. Am. **72**, (1), 156-160, (1982).

/2/ K. G. Larkin, D. Bone, and M. A. Oldfield, "Natural demodulation of two-dimensional fringe patterns: I. General background to the spiral phase quadrature transform.", To be published in J. Opt.Soc. Amer., A **18**, (8), tba, (2001).

/3/ K. G. Larkin, "Natural demodulation of two-dimensional fringe patterns: II. Stationary phase analysis of the spiral phase quadrature transform.", To be published in J. Opt.Soc. Amer., A **18**, (8), tba, (2001).

/4/ T. S. Kuhn, The Structure of Scientific Revolutions, 3rd, University of Chicago Press, Chicago, 1996.

/5/ B. Jahne, Practical handbook on Image processing for Scientific applications, CRC Press, Boca Raton, Florida, 1997.

/6/ K. G. Larkin, PhD Thesis, "Topics in Multi-dimensional Signal Demodulation", PhD. University of Sydney, 2001.

/7/ T. Bülow, D. Pallek, and G. Sommer, "Riesz Transforms for the Isotropic Estimation of the Local Phase of Moiré Interferograms," Symposium of the German Pattern Recognition Society (DAGM), Kiel, Germany, (2000), 333-340.

/8/ K. Andresen, and Q. Yu, "Robust Phase Unwrapping By Spin Filtering Combined With a Phase Direction Map", Optik **94**, (4), 145-149, (1993).

/9/ H. Canabal, J. A. Quiroga, and E. Bernabeu, "Local fringe direction calculation and application in moire deflectometry," Fringe '97, Bremen, Germany, (1997), 107-110.

/10/ J. L. Marroquin, R. Rodriguez-Vera, and M. Servin, "Local phase from local orientation by solution of a sequence of linear systems", J. Opt. Soc. Am., A **15**, (6), 1536-1544, (1998).

/11/ R. Penrose, "The topology of ridge systems", Ann. Hum. Genet.,Lond. **42**, 435-444, (1979).

/12/ D. C. Ghiglia, and L. A. Romero, "Robust Two-Dimensional Weighted and Unweighted Phase Unwrapping That Uses Fast Transforms and Iterative Methods", J. Opt. Soc. Am., A **11**, (1), 107-117, (1994).